Efficient material descriptions for modelling high-temperature processes

J H Zietsman[1,2]

[1]CEO, Ex Mente Technologies, Pretoria, South Africa, 0081. johan.zietsman@ex-mente.co.za
[2]Research Associate, Department of Materials Science and Metallurgical Engineering, University of Pretoria, Pretoria, South Africa, 0002

ABSTRACT

The transition to more sustainable metal production is receiving much attention at present, and the iron and steel industry is at the centre of the conversation. New, more environmentally friendly production technologies, such as DRI smelting furnaces, need to be developed in a short period of time. This necessitates increased use of computational modelling that incorporates more accurate material descriptions.

The combination of large-scale multiphysics models of high-temperature processes with CALPHAD material descriptions leads to infeasible computation times. This can be resolved with the previously reported RapidThermo framework, which has been demonstrated to make equilibrium calculations orders of magnitude faster, within controllable limits of accuracy.

In this paper, we explain how further material properties, which are important to modelling high-temperature reactors, can be added to the RapidThermo framework. This can improve the accuracy and usefulness of process and multiphysics models in the development of new technologies, which can significantly accelerate development cycles.

INTRODUCTION

To sustain and grow, modern society has a critical and growing need for metals to maintain and build infrastructure for accommodation, food production, transport, communication, etc. As we produce these metals, we emit waste and greenhouse gases that pollute water and the atmosphere, and influence the planet's climate, thereby threatening the very existence we aim to protect and expand. This is no longer a concern that lurks far into the future, but because governments have started to legislate emission reduction to combat climate change, it is a practical reality that we must face today. We need to find a balance between living, thriving, and growing, and destroying the environment without which we cannot exist.

To address this perceived existential threat, we need to change ... improve how we do things ... urgently. In pyrometallurgy this means we need to develop new processes that make better use of materials and energy, so that we can satisfy our needs for metals today, without destroying ourselves tomorrow.

Considering history, developing new high-temperature processes is difficult, costly, risky, and time-consuming. Given the magnitude and importance of this matter, though, it should be possible (1) to recruit talented people to take on these challenges and (2) to obtain the required funding. The two realities that remain are high risk and the time required. The scale and complexity of this challenge require that we learn at a high rate and fail many times, so that we can successfully get more efficient and sustainable processes into operation ... soon enough to protect our environment and ourselves.

To learn and develop new processes rapidly, we need to continue hypothesising, experimenting, and theorising, but faster than before, based on a greater reliance on computational methods. Physical measurements, experiments, and pilot-scale testing remain indispensable, but they are unlikely to yield the required pace on their own. Computer-based modelling (hypothesising) and simulation (experimenting) as the basis for developing new understanding (theorising) more realistically hold the potential for addressing the complexity and urgency of society's dilemma. Process and multiphysics models that describe the thermodynamics and kinetics of high-temperature processes and reactors

are crucial for improving the efficiency and profitability of existing operations, and for developing more sustainable production technologies.

Computational models in pyrometallurgy, although already useful today, are fundamentally constrained by how accurately and efficiently we can describe the materials involved. Thermochemical equilibrium calculations along with composition- and temperature-dependent properties of materials like slags, alloys, and mattes are mostly omitted from multiphysics models that can be used for design, operation, and new technology development. This is mainly because of the complexity and computational expense of (1) equilibrium calculations, and (2) solving partial differential equations (PDEs) influenced by varying, non-linear material properties. Directly integrating Gibbs energy minimiser routines into PDE solvers generally lead to infeasible computation times, specifically for systems of industrial interest.

In this paper we consider the current urgency to transition to "green steel" and the need to develop DRI smelting furnaces. Rapid development of such new technologies creates a greater need for computational modelling of high-temperature reactors, which in turn makes more accurate and computationally efficient material descriptions a necessity. We then consider the current realities and constraints of CALPHAD and multiphysics models and explain how the RapidThermo framework can contribute to making more detailed computational models of pyrometallurgical processes feasible.

REPLACING THE BLAST FURNACE

The iron and steel industry, the world's largest metallurgical industry by production volume, is the second-largest greenhouse gas emitter, and contributes 7 to 9 % of global CO_2 emissions. These emissions result mainly from producing pig iron with a blast furnace (BF) from iron ore and converting it to crude liquid steel with a basic oxygen furnace (BOF), as shown in Figure 1(a). This route emits close to 2 t CO_2/t liquid steel (LS) produced. Recycling scrap with the electric-arc furnace (EAF) route can emit as little as 0.13 t CO_2/t LS, but this route can provide neither the required volume nor all the required grades. (Wimmer, Fleischander and Voraberger, 2023)

(a) Traditional route.

(b) Proposed "green steel" route.
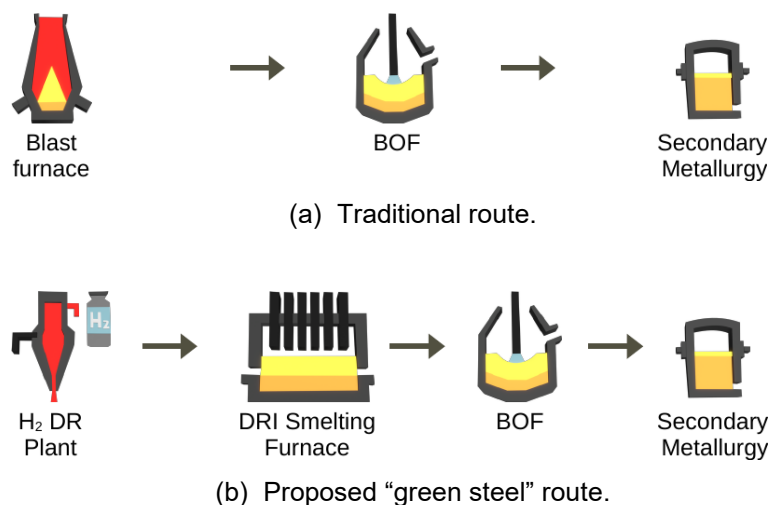
Figure 1: Process routes for converting abundant low-grade iron ore to liquid steel. (Reproduced from Wimmer, Fleischander and Voraberger, (2023).)

Directly reducing high-grade iron ore with hydrogen to produce H_2-DRI and melting it down in an EAF can yield as low as 0.2 t CO_2/t LS. Economically viable processing of low-grade iron ore, which is most abundantly available, into liquid pig iron via direct reduction requires a semi-continuous DRI smelting furnace (DSF), however, as shown in Figure 1(b). (Wimmer, Fleischander and Voraberger, 2023) DSF technology does not currently exist, and is currently a point of much attention in the iron and steel industry.

Some European countries, like the Netherlands and Germany, have legislated strict deadlines for the steel industry to adhere to. In some cases, DRI-DSF technology, with DSF units operating at about 100 MW to produce 1 Mt pig iron/a, needs to be operational by 2030, which leaves little time for developing the DSF concept into a successfully operating production technology.

DRI Smelting

Several questions need to be answered to develop and ultimately design DSFs. These include:

1. What type of furnace should be used? E.g. rectangular 6-electrode AC, circular 3-electrode AC, circular single-electrode DC as shown in Figures 2(a) to 2(c).

2. How should energy be discharged into the process? E.g. Immersed electrode(s), brush arc(s), open arc(s) as shown in Figures 2(d) to 2(f).

3. What configuration should the furnace power supply have? E.g. number of taps, tap voltages, resistance, current.

4. Where should feed be discharged into the process? E.g. Close to the walls, close to the electrode(s) as shown in Figures 2(g) and 2(h).

5. What will the furnace's energy consumption and efficiency be?

6. How should the process be contained? E.g. Slag saturated in refractory components, sidewall feed heaps, slag freeze lining as shown in Figures 2(g) and 2(h).

7. What will the furnace's production capacity be? E.g. 1 Mt/a of tapped alloy.

8. What will the composition of the liquid alloy product be? Carbon and silicon contents are of specific importance for the downstream BOF process.

(a) Rectangular 6-in-line AC furnace.

(b) Circular 3-electrode AC furnace.

(c) Circular single-electrode DC furnace.

(d) Immersed electrode.

(e) Brush arc.

(f) Open arc.

(g) Side feeding and sidewall feed heap containment.

(h) Centre feeding and slag freeze lining containment.
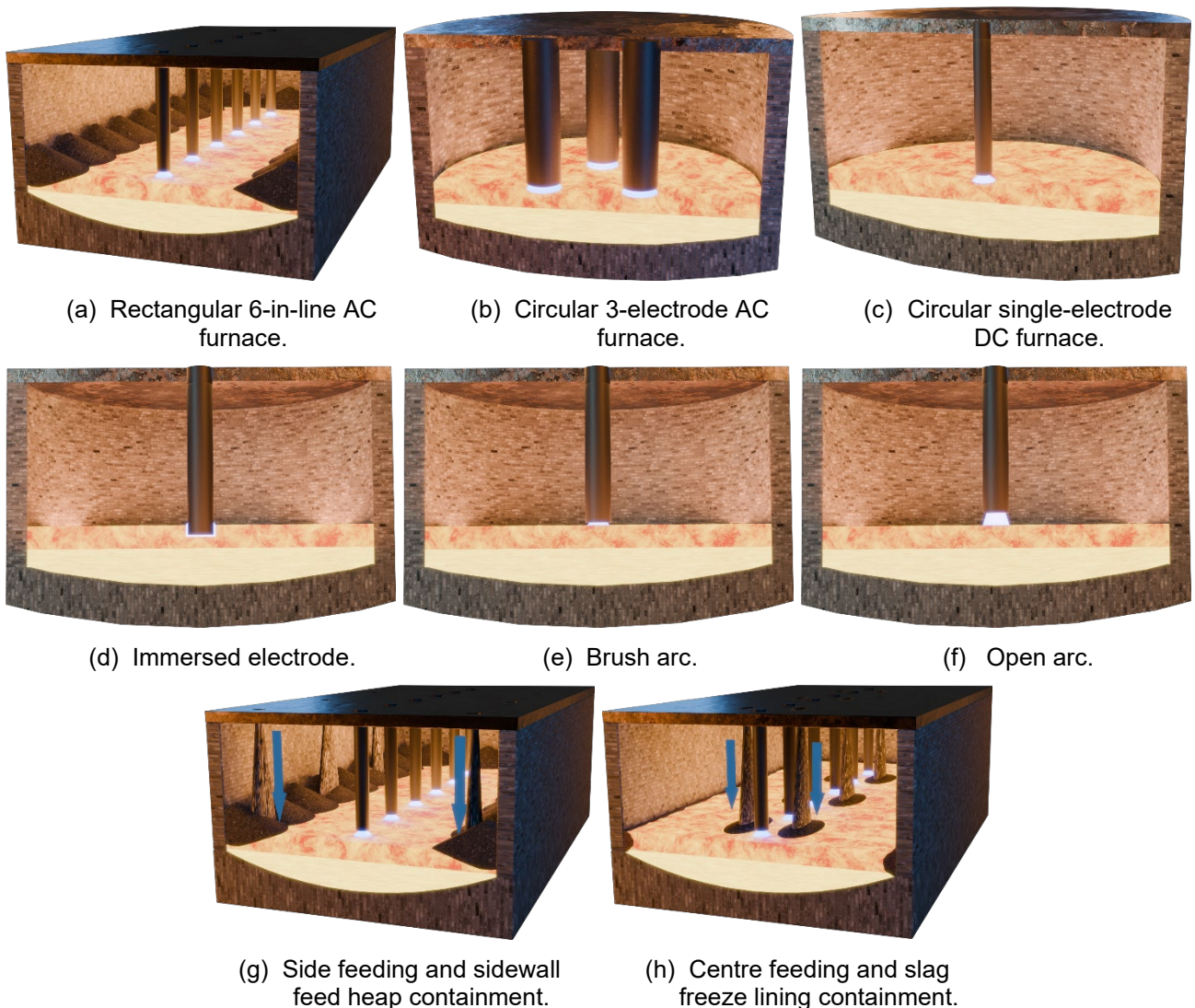
Figure 2: Equipment and design choices relevant to DRI smelting furnaces.

Question 5 is easiest to answer based on mass and energy balance calculations and a heat transfer model of the furnace. Questions 1 to 4 are often driven by an equipment supplier's experience and capabilities, and by operational and scale considerations, and their answers have implications for questions 5 to 8. Questions 6 to 8 (the Key Questions) are the most difficult to answer. They are influenced by the preceding questions, and, very importantly, also by feed material properties, furnace operating conditions, and process material properties.

The development tasks are interdependent – furnace design depends on the process, which depends on material properties and operating conditions, which depend on raw materials and furnace design. To solve the problem, it is therefore necessary to iterate through different furnace designs, operating conditions, and process material compositions to converge to a configuration that will operate successfully. Within the time constraints, research and development iterations can feasibly involve laboratory experiments, and focused but limited pilot-scale testing. Extensive pilot-scale testing and demonstration-scale operation appear to be out of the question. It is therefore reasonable to conclude that computational modelling and simulation need to contribute substantially to DSF development for such furnaces to be in operation by 2030 or soon after.

Modelling a DSF

We can use process models to describe mass and energy balances (Zietsman, Steyn and Pretorius, 2018) and study dynamic process behaviour (Zietsman and Pistorius, 2006), thereby answering some of the questions posed in the previous section. The Key Questions require that we use multiphysics models to investigate the influences of and interactions between geometry, scale, transport phenomena, and material properties.

Table 1 and Figure 3 indicate the scope and complexity of a DSF multiphysics modelling endeavour, focusing only on the most important aspects – it is an ambitious task. The model needs to describe several physical phenomena, which involve several materials, as functions of varying temperature and composition. This means that a wide range of material property models are needed.
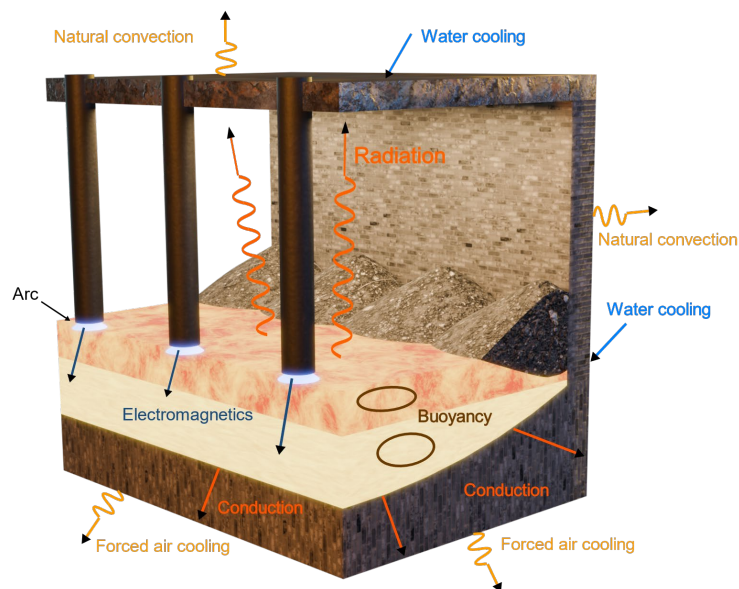
Figure 3: Physical phenomena important to DSF modelling, design, and operation.

In the case of the slag bath (column highlighted in Table 1), for example, electrical current flow and joule heating release energy, which is transported through thermal conduction and fluid flow driven by buoyancy and Lorentz forces. Chemical reactions and phase change occur, which involve DRI, reductant, and flux particles, liquid and solid slag, liquid and solid alloy, and gas. Considering only the liquid slag material (row highlighted in Table 1), descriptions of density, heat capacity, Gibbs energy, magnetic permeability, electrical conductivity, thermal conductivity, and viscosity are required.

Table 1: Most important phenomena, materials, and material properties relevant to DSF multiphysics modelling. Most properties vary with temperature and composition. Gibbs energy $\bar{G}$ collectively refers to material thermodynamic properties, which also include $\bar{S}$ and $\bar{H}$. The slag bath region column and liquid slag material row are emphasised in blue.

Phenomenon	EA	SB	AB	FB	FL	FH	Thermodynamic	Kinetic
Electromagnetics								
Magnetohydrodynamics	✓	✓	✓				ρ	$\mu_{\mathrm{m}}\,\sigma\mu$
Electrical current flow	✓	✓	✓					σ
Joule heating	✓	✓	✓					σ
Heat Transfer								
Thermal conduction	✓	✓	✓	✓	✓	✓	$\rho\,\bar{C}_P$	κ
Thermal radiation				✓				$\alpha_{\mathrm{r}}\,\rho_{\mathrm{r}}\,\tau_{\mathrm{r}}$
Momentum Transfer								
Fluid flow		✓	✓	✓			ρ	μ
Buoyancy		✓	✓	✓			ρ	
Lorenz forces		✓	✓					$\mu_{\mathrm{m}}\,\sigma$
Chemical Changes								
Chemical reactions		✓			✓	✓	$\bar{G}$	
Phase change		✓	✓		✓		$\bar{G}$	

Material	EA	SB	AB	FB	FL	FH	Thermodynamic	Kinetic
Raw Materials								
DRI particles		✓				✓	$\rho\,\bar{C}_P\,\bar{G}$	κ
Reductant particles		✓				✓	$\rho\,\bar{C}_P\,\bar{G}$	κ
Flux particles		✓				✓	$\rho\,\bar{C}_P\,\bar{G}$	κ
Process Materials								
Liquid slag		✓			✓	✓	$\rho\,\bar{C}_P\,\bar{G}$	$\mu_{\mathrm{m}}\,\sigma\,\kappa\,\mu$
Solidified slag		✓			✓	✓	$\rho\,\bar{C}_P\,\bar{G}$	κ
Liquid alloy		✓	✓			✓	$\rho\,\bar{C}_P\,\bar{G}$	$\mu_{\mathrm{m}}\,\sigma\,\kappa\,\mu$
Solidified alloy		✓	✓			✓	$\rho\,\bar{C}_P\,\bar{G}$	κ
Freeboard Materials								
Dust	✓			✓		✓	$\rho\,\bar{C}_P\,\bar{G}$	$\alpha_{\mathrm{r}}\,\rho_{\mathrm{r}}\,\tau_{\mathrm{r}}$
Fume	✓			✓			$\rho\,\bar{C}_P\,\bar{G}$	$\alpha_{\mathrm{r}}\,\rho_{\mathrm{r}}\,\tau_{\mathrm{r}}$
Gas	✓	✓		✓		✓	$\rho\,\bar{C}_P\,\bar{G}$	$\alpha_{\mathrm{r}}\rho_{\mathrm{r}}\tau_{\mathrm{r}}\kappa\,\mu$
Others								
Plasma	✓			✓			$\rho\,\bar{C}_P$	$\sigma\,\kappa\,\mu$

EA: electric arc, SB: slag bath, AB: alloy bath, FB: freeboard, FL: slag freeze lining, FH: sidewall feed heap

COMPUTATIONAL REALITIES

When considering comprehensively addressing the scope in Table 1 and focusing on liquid slag and other oxide phases in particular, we are confronted with a number of realities, which are true in the case of DSFs, but also in many, if not most, other pyrometallurgical scenarios.

Thermodynamic Space

The Gibbs phase rule shown in Equation (1) shows the number of dimensions in which materials exist, and therefore the number of dimensions that we need to perform calculations in. A system's dimensionality is equal to $\hat{\mathfrak{f}}^{\rho}$ with $\hat{\varphi}^{\rho} = 1$.

$$\hat{f}^{\rho} = \hat{\psi}^{\rho} + \hat{\varepsilon}^{\sigma} + \sum_{i=1}^{\hat{\varphi}^{\rho}} \hat{\varepsilon}^{\varphi_i} - \hat{\varphi}^{\rho} - \hat{\zeta}^{\sigma} - \sum_{i=1}^{\hat{\varphi}^{\rho}} \hat{\zeta}^{\varphi_i} \tag{1}$$

In pyrometallurgy we usually work at constant pressure and varying temperature ($\hat{\psi}^{\sigma} = 1$), and with large numbers of system components. In the case of a DSF, iron ore combined with carbonaceous reductants commonly contain Al, C, Ca, Fe, H, K, Mg, Mn, N, Na, O, P, S, Si ($\hat{\varepsilon}^{\sigma} = 14$), when ignoring other minor elements. Assuming that there are no compositional constraints ($\hat{\zeta}^{\sigma} = \hat{\zeta}^{\varphi_i} = 0$), these elements combine with temperature to yield $\hat{f}^{\rho} = 14$ when $\hat{\varphi}^{\rho} = 1$ ... a 14-dimensional system. This results in the "curse of dimensionality", which exponentially increases the required computation, memory, and storage space as the number of dimensions increase.

As an example, when generating a grid with 25 points in each dimension and storing the necessary independent and dependent parameters (each represented by a single double-precision floating point number of 8 B) at each grid location will require 17.50 to 144.5 TB of storage space. Such a data set will only sparsely cover the 14D domain and it will not capture detailed phase diagram features. Table 1 shows that values for several material thermodynamic properties (MTPs) and material kinetic properties (MKPs) need to be stored, and each of these will further increase the required storage space. In comparison, the GPT-4 large language model (LLM) used a dataset with 1 T tokens, and has about 1.76 T parameters (OpenAI, 2023; The Decoder, 2023). (These figures were not formally released by OpenAI but are provided as a relatable reference.)

Training a large neural network that can describe the example DSF system with all its thermodynamic and kinetic properties is possible in principle, but the enormity of thermodynamic space makes it practically infeasible. Exorbitant amounts of data (measured or calculated), computation, memory, and storage space would be required.

The Limits of Computation

When building a multiphysics model for answering the Key Questions related to DSF technology, we are primarily describing transport phenomena, and are therefore heavily dependent on kinetic properties. These properties are influenced by thermodynamic properties, which are determined by equilibrium behaviour as determined with Gibbs energy minimisation (GEM) calculations at the temperatures and compositions inside a DSF. These aspects are interdependent, which makes it necessary to solve such a model iteratively.

Roos and Zietsman (2022, Fig. 2) showed that direct integration of GEM calculations with up to 10 system components into realistically sized multiphysics models can result in computation times of up to hundreds of years for modest numbers of iterations. These durations only allowed for equilibrium calculations, and not for further material property calculations. Therefore, integrating partial differential equation (PDE) solver software and GEM software that are available today, yields infeasible computation times. This infeasibility is the thrust behind developing the RapidThermo material description framework (Roos and Zietsman, 2022).

The same authors showed that the burden of calculating and storing data across a DSF's entire 14D domain can be reduced in two ways. Firstly, the Gibbs phase rule reduces the number of dimensions by ($\hat{\varphi}^{\rho} - 1$) (Roos and Zietsman, 2022). For example, when liquid alloy, liquid slag, dicalcium silicate, and gas are stable, it is only necessary to work in 11 dimensions rather than 14. Secondly, only those regions of the phase diagram in which the process in question is active need to be populated with in-situ tabulation (Roos, Bogaers and Zietsman, 2023). This is demonstrated in Figure 4 with simplified compositional spaces for ironmaking, steelmaking, and ilmenite smelting, which shows that large regions of compositional space will likely be unimportant for simulating such processes.
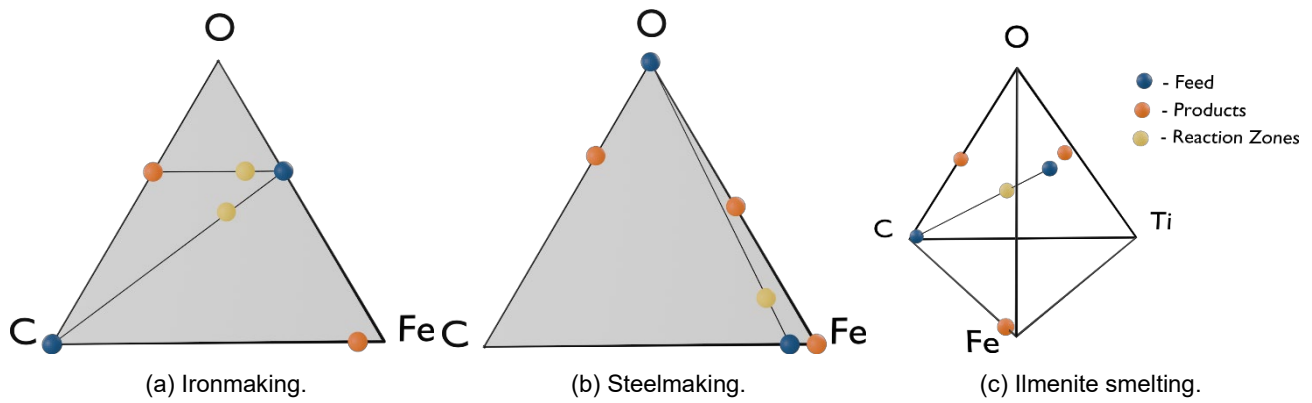
Figure 4: Simplified compositional spaces indicating regions that need to be considered to describe feed and product materials, and process reaction zones.

Thermodynamic Properties

The thermodynamic behaviour (G, S, H) of the example 14D DSF system are fairly well (but not perfectly) described with thermochemical data in CALPHAD software such as FactSage (Bale et al., 2016). There are still regions of this system that are not well described, or described at all by the available data. Calculating the equilibrium state of a system through GEM with such software is possible, but too slow for doing large numbers of calculations in short periods of time.

$\bar{C}_p, \Delta \bar{H}_{\mathrm{f},298K}$ and $\bar{S}_{298K}$ of pure substances and $\bar{G}$ of solutions are described reasonably well in CALPHAD software databases. Recent progress has been made with the description of molar volume and thermal expansivity that together describe density with a CALPHAD model (Thibodeau, Gheribi and Jung, 2016a; Thibodeau, Gheribi and Jung, 2016b; Thibodeau, Gheribi and Jung, 2016c) and density functional theory (DFT) (Liu, Wang and Shang, 2022) models, but these models are not yet readily available in CALPHAD software. Because density differences drive flow through buoyancy, better descriptions of slag density can contribute to more accurate simulation of fluid flow and heat transfer in a DSF slag bath with multiphysics models.

Kinetic Properties

When considering silicate slags relevant to the example 14D DSF system, the best described kinetic property is viscosity, with several models available in CALPHAD software or based on CALPHAD solution models (Grundy et al., 2008; Kim, 2011; Wu et al., 2015). Thibodeau and Jung (2016) reported a structure-based electrical conductivity model for slags. A similar model for thermal conductivity is not currently available. These properties combine to influence energy discharge, fluid flow, and heat transfer, all of which are relevant and important to developing DSFs.

General practice in multiphysics modelling is to select single values for these properties, and keep them constant throughout a simulation, without accounting for the influences of changing temperature and composition in a furnace over time. This is one of the core reasons why multiphysics models can only describe high-temperature systems with limited accuracy. To improve these models, these kinetic properties (μ, σ, and κ) need to be integrated along with thermodynamic properties and phase states at equilibrium. Accomplishing this through direct integration of CALPHAD and multiphysics software is infeasible at present.

Summary

The challenges stated above can be summarised as follows:

1. It is infeasible to cover the vast thermodynamic space of a DSF process by pre-calculating data and, for example, fitting a neural network.

2. It is infeasible to use direct integration of equilibrium calculations in multiphysics models.

3. It is possible to calculate some thermodynamic properties with CALPHAD tools, but due to the dependence on equilibrium calculations, this is infeasible for high-throughput computation.

4. It is possible to calculate some kinetic properties of a system with CALPHAD tools, but due to the dependence on both equilibrium calculations and thermodynamic properties, it remains infeasible for high-throughput computation.

This leads to the conclusion that high-fidelity, high-resolution simulation of pyrometallurgical processes of industrial importance is currently infeasible. As shown in Table 2, the RapidThermo accelerator framework development by Roos and Zietsman (2022) addresses item 1 above through dimensional reduction and in-situ tabulation, item 2 through tabulation of equilibrium calculation results, and item 3 partially through tabulation of phase thermodynamic properties.

Table 2 – Current capabilities related to material property determination, description, and application. Shaded cells show the scope targeted by the RapidThermo framework.

Property	Property Determination	CALPHAD Descriptions	Efficient Descriptions	Dependent Models
	Properties can be determined with physical measurements; computation, e.g. DFT, MD.	Descriptions are readily available in CALPHAD software.	Sufficiently efficient descriptions are available for high-throughput computation.	Models that depend on these properties and descriptions.
Pure Substances / Pure Phases (PPs)				
Structural properties				
- Crystal structure	✓	✓		MP(SP)
- Atomic/ionic radii	✓	✗		MP(SP)
Thermodynamic properties				
- $\bar{S}_{298K}\ \bar{C}_P\ \bar{G}$	✓	✓	✗	MP(TP) GM
- $\bar{V}\ \alpha_V\ \rho$	✓	-	✗	MP(TP) GM
Kinetic properties				
- $\mu\ \sigma\ \kappa$	✓	✗	✗	MP(KP) MP
Solution Phases / Mixture Phases (MPs)				
Structural properties				
- Crystal structure	✓	✓		MP(TP,KP)
- Atomic/ionic radii	✓	✗		MP(TP,KP)
- Inter-atomic/ionic distances	✓	✗		MP(KP)
Thermodynamic properties				
- $\bar{S}°\ \bar{H}°\ \bar{G}^{ex}$	✓	✓	✓	GM PR MP
- $\bar{V}°\ \bar{V}^{ex}\ \alpha_V\ \rho$	✓	✗	✗	MP
Kinetic properties				
- μ	-	✓	✗	MP
- $\sigma\ \kappa$	-	✗	✗	MP
Equilibrium State				
System properties				
- Phase fractions	✓	✓	✓	SP(TP,KP) PM MP
- Thermodynamic quantities	✓	✓	✓	PM MP
Phase properties				
- Molar composition	✓	✓	✓	PM MP
- Thermodynamic quantities	✓	✓	✓	PM MP
Morphology				
- particle size, surface area	✗	✗	✗	CM(KP) MP
Apparent TPs				
- $\check{H}\ \check{C}_P$		✓	✓	PR MP
- $\bar{V}\ \alpha_V\ \rho$		✗	✗	MP
Apparent kinetic properties				
- $\mu\ \sigma\ \kappa$		✗	✗	MP

SP: structure property TP: thermodynamic property KP: kinetic property

MP: multiphysics models PR: process models GM: Gibbs energy minimisation

CM: composite material (multiple phases)

✓: good -: ok ✗: bad

The following can also be noted based on Table 2.

1. Pure substances:

   Properties can be determined by experimental measurement and, more recently, with computational chemistry (Liu, Wang and Shang, 2022). CALPHAD descriptions provide crystal structure information, but not dimensions such as atomic/ionic radii, or kinetic properties. The latter is improving in, for example, FactSage (Bale et al., 2016). The available descriptions are not suitable for direct inclusion in high-throughput computations such as multiphysics models.

2. Solution phases:

   Determining structure information, thermodynamic properties, and kinetic properties with physical measurements is possible but generally difficult for slags. Computational chemistry (e.g. DFT, MD) has made progress with determination of kinetic properties (Mongalo, Lopis and Venter, 2016), but much is still left to do. CALPHAD descriptions provide structure information, but not dimensional information, and not yet all required thermodynamic, and kinetic property descriptions. The available descriptions are not suited for high-throughput computation.

3. Equilibrium state:

   System and phase properties are described well with CALPHAD models, and these can be integrated into high-throughput computations with RapidThermo. Morphology influences the kinetic properties of composite materials (e.g. viscosity of slag with dispersed solids). This cannot be addressed with CALPHAD software at all because morphology is not determined by equilibrium. Some thermodynamic properties, and all the required kinetic properties are not yet accessible in high-throughput computation.

Continued RapidThermo development to incorporate further thermodynamic properties (item 3) and kinetic properties (item 4) is the focus of the next section.

EFFICIENT MATERIAL DESCRIPTIONS

Figure 5 shows that the RapidThermo accelerator accepts an independent system state $\mathbf{X}^{\sigma}$ as input. It returns a dependent equilibrium system state $\mathbf{Y}^{\sigma}$ directly calculated by CALPHAD software as result if its database contains insufficient data but returns interpolated values $\widetilde{\mathbf{Y}}^{\sigma}$ once enough data is available. The database is populated *in situ*, which means it can start empty and be populated as the connected process or multiphysics models request calculation results; there is no need for a large number of pre-calculations. The interpolation routine is substantially faster than GEM calculations, and the benefit grows as the number of system components increases (Roos, Bogaers and Zietsman, 2023). This makes incorporating accurate material descriptions into such models more feasible.

The accelerator discretises the system's phase diagram, which is 14-dimensional in the DSF example, into small thermochemical cells within which it can use interpolation based on the lever rule to calculate $\widetilde{\mathbf{Y}}^{\sigma}$ results, which limits expensive CALPHAD software calculations. To be clear though, the RapidThermo accelerator does not aim to replace or eliminate the use of CALPHAD software. It acts as an intermediary between computationally intensive models and CALPHAD software to make more detailed, more accurate, and larger-scale investigation of pyrometallurgical processes feasible.

The core requirements of the RapidThermo algorithm are:

1. Configurability: The accelerator must

   o be generic, so that it can function for any number of system components and nonchemical potentials;

   o use minimal configuration, including thermochemical system data and metadata, and discretisation ranges and cell sizes; and
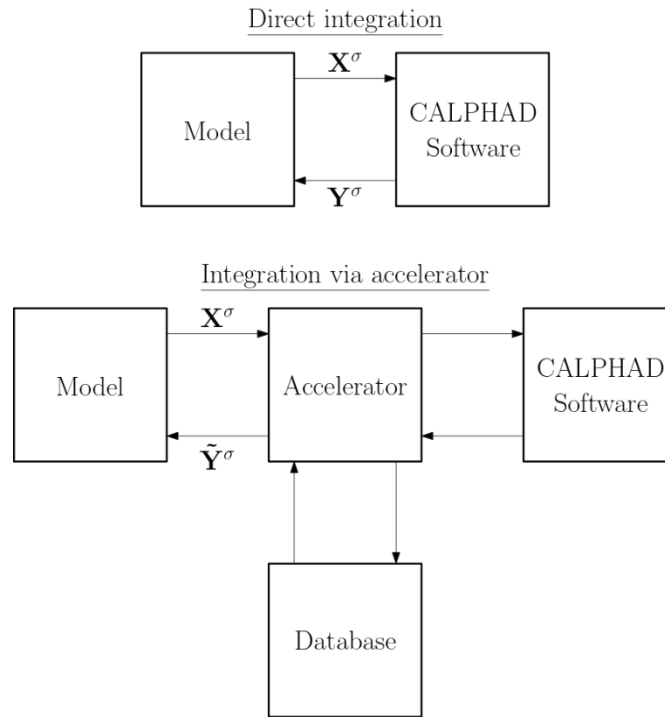
FIG 1: The RapidThermo accelerator concept compared with direct integration between models and CALPHAD software (indicated as equilibrium calculation software). (Roos and Zietsman, 2022)

- o be modular, to allow changing sub-algorithms for discretisation, interpolation, and multiphase property calculation by changing configuration settings rather than changing source code.

2. Efficiency: The accelerator must

- o perform calculations orders of magnitude faster than the CALPHAD software it integrates with, to allow feasible solution of the connected process and multiphysics models;

- o allow parallel execution, so that large numbers of $\mathbf{X}^\sigma$ can be specified and large numbers of $\mathbf{Y}^\sigma$ can be returned simultaneously; and

- o require minimal computer memory and storage space to allow execution on reasonably-costed computer hardware.

3. Accuracy: The accelerator must

- o produce calculation results that satisfy mass, element mass, and energy conservation within machine precision; and

- o allow control over interpolation accuracy through configuration of discretisation cell ranges and sizes.

Table 2 shows that the accelerator reported by Roos, Bogaers and Zietsman (2023) can calculate system phase fractions and thermodynamic quantities, phase molar compositions and thermodynamic quantities, as well as $\bar{C}_p$ and $\Delta \bar{H}_P$ for combinations of multiple phases. These capabilities allow more sophisticated multiphysics model calculations that can describe, for example, phase change associated with slag freeze linings.

As indicated in Table 1, further properties that are required to describe DSFs include density, viscosity, electrical conductivity, and thermal conductivity, for both single phases such as liquid slag and multiple phases. Similar to $\bar{C}_p$ and $\Delta \bar{H}_P$, these properties only need to be stored in single phase regions and on one-phase-fraction (OPF) boundaries for single phases. This has the benefit of reducing the number of data points that need to be calculated and stored. These properties are further addressed in the remainder of this section, with specific reference to liquid slag.

Slag Structure

When oxides melt and mix to become a liquid slag, the cations and anions will with time arrange themselves into the most probable, or equilibrium, configuration Γ_{eq}^{σ}. Considering a binary CaO-SiO$_2$ melt, Si-O-Si bonded oxygen ions are indicated as O^0 and referred to as bridged oxygens, Ca-O-Ca bonded ones are indicated as O^{2-} and referred to as free oxygens, and Ca-O-Si bonded ones are indicated as O$^-$ and referred to as broken oxygens. The structure of this melt can be described with Q^0, Q^1, Q^2, Q^3, Q^4, and Ca-Ca species; the superscript indicates the number of oxygen atoms per Si tetrahedron that binds to another Si atom. The equilibrium mole fractions of the different species change with composition and temperature, and can be determined experimentally or with CALPHAD software such as FactSage. (Thibodeau, Gheribi and Jung, 2016a)

The structure of the melt directly influences its properties, such as molar volume, thermal expansivity, viscosity, electrical conductivity, and thermal conductivity. Some property models use equilibrium structure information from the Modified Quasichemical Model (MQM) (Pelton and Blander, 1986) in FactSage to estimate property values (Grundy et al., 2008; Thibodeau, Gheribi and Jung, 2016a; Thibodeau and Jung, 2016). Calculated equilibrium structure data would be too large to efficiently store in RapidThermo. This data must therefore be used to calculate property values, which can be stored efficiently, and then discarded.

Slag Properties

Density, viscosity, electrical, and thermal conductivity are the most important properties that need to be accessible to multiphysics models, of DSFs for example. This additional information must be provided by RapidThermo at the lowest possible additional computational, memory, and storage cost.

Density

Phase density (Equation (2)) varies with composition and temperature; it is determined by molar volume (Equation (3)) and thermal expansivity (Equation (4)).

$$\rho^{\varphi} = \frac{\sum_{\mu=1}^{\hat{\mu}_{\mu}^{\varphi}} x_{\mu}^{\varphi} \bar{m}_{\mu}}{\bar{V}^{\varphi}} \tag{2}$$

$$\bar{V}^{\varphi} = \frac{V_{T_{ref}^{\varphi}}^{\varphi}}{\sum_{\mu=1}^{\hat{\mu}^{\varphi}} n_{\mu}^{\varphi}} \left(1 + \alpha_{V}^{\varphi}(T - T_{ref})\right) \tag{3}$$

$$\alpha_{V}^{\varphi} = \frac{1}{\bar{V}^{\varphi}} \frac{\partial \bar{V}^{\varphi}}{\partial T} \tag{4}$$

Liquid slag density can be calculated either directly based on structure data from GEM results and the model by Thibodeau, Gheribi and Jung (2016c), or interpolated with previously calculated data stored in the RapidThermo database. It is sufficient to store only ρ^{slag} rather than both $\bar{V}^{slag}$ and α_{V}^{slag}, since the accelerator's discretisation scheme will implicitly store both composition and temperature dependence.

Density of a mixture of phases is not dependent on morphology. The combined density of the phases ρ can therefore be determined simply with Equation (5), based on either directly calculated or interpolated single-phase densities ρ^{φ}, which obviates storage of multi-phase density data.

$$\rho = \frac{m^{\sigma}}{\sum_{\varphi=1}^{\hat{\phi}^{\rho}} \frac{m^{\varphi}}{\rho^{\varphi}}} \tag{5}$$

Viscosity

Single-phase dynamic viscosity μ^{φ} is only relevant to fluids such as gas, liquid slags, and liquid alloys. Together with the flow domain geometry, it determines the rate at which momentum is transferred. This is important for fluid flow and heat transfer in high-temperature reactors such as DSFs. Liquid slag viscosity can be calculated with models from Grundy et al. (2008), Kim (2011) and Wu et al. (2015), all of which use structure data from GEM calculations as basis.

Because viscosity is a kinetic property, the morphology of a mixture of phases influences the mixture's apparent viscosity μ (Schupsky et al., 2020). In the case of a single liquid phase with suspended solid phases, the Einstein-Roscoe equation (Roscoe, 1952) is often used (Equation (6)). This equation omits the influence of solid particle morphology, and therefore the interfacial area between liquid and solid phases.

$$\mu^{\mathrm{apparent}} = \mu^{\mathrm{liquid}} \left(1 - 1.35 \frac{V^{\mathrm{solids}}}{V_{\mathrm{liquid}}} \right) \tag{6}$$

When the phase mixture only consists of liquids, such as a molten slag and alloy, Equation (7) can be used to calculate apparent viscosity as a volume weighted average (Muller, Zietsman and Pistorius, 2015), which also ignores morphology.

$$\mu^{\mathrm{apparent}} = \frac{1}{V^{\sigma}} \sum_{\varphi=1}^{\hat{\varphi}^{\rho}} V^{\varphi} \mu^{\varphi} \tag{7}$$

Electrical Conductivity

Single-phase electrical conductivity σ^{φ} together with domain geometry, and the electrical potential field determine the rate at which electrical charge is transferred. This releases energy through joule heating, which drives subsequent heat transfer, in high-temperature reactors such as DSFs. Liquid slag electrical conductivity can be calculated with the model from Thibodeau and Jung (2016), which uses equilibrium structure data as basis.

As a kinetic property, the morphology of a mixture of phases influences the mixture's apparent electrical conductivity $\sigma^{\mathrm{apparent}}$. When ignoring morphology, an average weighted by volume fractions can be used as a simple approximation.

$$\sigma^{\mathrm{apparent}} = \frac{1}{V^{\sigma}} \sum_{\varphi=1}^{\hat{\varphi}^{\rho}} V^{\varphi} \sigma^{\varphi} \tag{8}$$

Thermal Conductivity

Thermal conductivity is the slag property that is most lacking in data and models. It is also of great importance to new technologies such as DSFs, since energy released through electrical heating must be transported, at least in part, through the slag bath. We suspect that heat transfer rates through the slag bath may be the fundamental capacity constraint of these new processes.

It may be possible to resolve some of these problems with computational methods such as MD and DFT for single phases. Multiple phases can be approached similar to electrical conductivity, due to the similarities between the two properties.

Summary

The availability of sophisticated material property models based on slag structure makes it feasible and relatively simple to add thermodynamic and kinetic material properties to the information stored by the RapidThermo framework. These models use equilibrium calculation results as basis and compute physical properties at limited additional cost. The calculated properties only need to be stored on OPF boundaries, as is the case with the compositions, heat capacities, and enthalpies of single phases.

Electrical conduction in slags involves transport of charge with ions and electrons (Equation (9)). Similarly, slag thermal conduction involves transport of heat with phonons (lattice vibrations), photons (thermal radiation), and electrons (Equation (10)). MQM structure information is used successfully as basis for describing σ_{ion}^{slag} (Thibodeau and Jung, 2016), and may similarly be able to support

calculation of κ_{phn}^{slag}. It does not provide sufficient information, though, for estimating electronic and radiation components. It is therefore not yet possible to describe high-TiO_2 slags, for example, that have large electronic contributions to their electrical and thermal conductivities.

$$\sigma^{slag} = \sigma_{ion}^{slag} + \sigma_{elc}^{slag} \tag{9}$$

$$\kappa^{slag} = \kappa_{phn}^{slag} + \kappa_{elc}^{slag} + \kappa_{pht}^{slag} \tag{10}$$

All multiphase properties are re-calculated efficiently with interpolation based on density information and the lever rule, which obviates the need for excessive storage. Simple volume-based multiphase descriptions can be exchanged for more sophisticated models when morphology information is available. Simple descriptions can already improve multiphysics models significantly compared with assuming constant material property values.

Even though RapidThermo stores the minimum amount of data required for adequately accurate material descriptions, memory and storage requirements may increase to infeasible levels. In such cases, artificial neural networks (ANNs) may be fitted on OPF data to provide drastically compressed phase boundary descriptions. Such non-linear fits will have to be constrained to ensure that they remain thermodynamically consistent, and that mass, element mass, and energy conservation are still adhered to.

CONCLUSION

The pressure to develop new production technologies for the iron and steel industry is clear, and a current reality. If DRI smelting furnaces are to be in successful operation as soon as 2030, computational modelling will have to play a large part in the development process. This, in turn, needs more comprehensive, accurate, and computationally efficient material descriptions as a crucial component. Combining multiphysics models and existing material descriptions with existing methods and software will, however, lead to infeasible computation times.

It has been demonstrated in earlier work that the RapidThermo framework can capture equilibrium phase compositions, heat capacity, and enthalpy, which can make substantially faster material descriptions available for process and multiphysics models. In this paper we explained how other material properties, including density, viscosity, electrical conductivity, and thermal conductivity can be added to the framework, to make more realistic models of high-temperature reactors possible.

The current work identified the following points for further investigation:

1. Large memory and storage requirements on OPF boundaries may make it necessary to compress this data. Artificial neural networks may provide a feasible solution, especially since large amounts of data would be available.

2. Solution models like the MQM do not yet provide sufficient information to describe the electronic components of electrical and thermal conduction, and the radiation component of thermal conduction. It may be useful to extend such models to produce additional structure, geometric and dimensional information that can be used as basis for estimating these properties.

ACKNOWLEDGEMENTS

NOMENCLATURE

Extensive Variables			Intensive Variables		
U	internal energy	J			
S	entropy	JK^{-1}	T	temperature	K
V	volume	m^3	P	pressure	Pa
H	enthalpy	J			
G	Gibbs energy	J			
n	amount of substance	mol	μ	chemical potential	$J\,mol^{-1}$
			x	amount fraction	$mol\,mol^{-1}$
m	mass	kg	y	mass fraction	$kg\,kg^{-1}$

Arrays are indicated with boldface. E.g. **n** is an array of n_i.

Extensive Variable Modifier Notation

$\bar{V}$	integral molar	V/n	$\hat{V}$	partial molar	$\dfrac{\partial V}{\partial n_i}$
$\check{V}$	integral mass-specific	V/m			

Material Thermodynamic Properties / Material Kinetic Properties

Material Thermodynamic Properties			Material Kinetic Properties		
$\bar{C}_P$	heat capacity	$J\,K^{-1}\,mol^{-1}$	μ	dynamic viscosity	$Pa\,s$
	molar volume	$m^3\,mol^{-1}$	σ	electrical conductivity	$S\,m^{-1}$
	thermal expansivity	K^{-1}	κ	thermal conductivity	$W\,m^{-1}\,K^{-1}$
	mass density	$kg\,m^{-3}$	μ_m	magnetic permeability	$H\,m^{-1}$
			α_r	thermal radiation absorptivity	$W\,W^{-1}$
			ρ_r	thermal radiation reflectivity	$W\,W^{-1}$
			τ_r	thermal radiation transmissivity	$W\,W^{-1}$

Objects Related to Thermochemistry

Υ	the universe		ς	the surroundings
σ	the system		ρ	phase region (unique set of phases) in a phase diagram
Γ^σ	a macrostate (macroscopic configuration) of σ		f	a degree of freedom
Γ^σ_{eq}	an equilibrium state of σ		φ	a phase
γ^Γ	a microstate (microscopic configuration) of Γ		ε^φ	a component, e.g. an element or electron, local to φ
ψ^σ	a non-chemical potential of σ, e.g. T, P		ζ^φ	a compositional constraint of φ
ε^σ	a component (usually chemical element) of σ		ϵ^φ	an independent component of φ
ζ^σ	a compositional constraint of σ		μ^φ	a constituent of φ
ϵ^σ	an independent component of σ		λ^φ	a sublattice of φ
			μ^λ	a constituent of λ

Hat notation indicates "the number of" an object. E.g. $\hat{\varphi}^\rho$ is the number of phases in a phase region.

REFERENCES

Bale, CW et al. (2016). "FactSage Thermochemical Software and Databases – 2010 - 2016". In: *Calphad* 55.1 (0364-5916), pp. 1–19. doi: 10.1016/j.calphad.2016.07.004.

Grundy, A N et al. (2008). "A model to calculate the viscosity of silicate melts. Part I: Viscosity of binary SiO_2-MeO_x systems (Me = Na, K, Ca, Mg, Al)". In: *International Journal of Materials Research* 99.11, 1185–1194. doi: 10.3139/146.101752.

Kim, W-Y (2011). "Modelling viscosity of molten slags and glasses". Ph.D. Ecole Polytechnique de Montréal.

Liu, Z-K, Y Wang and S-L Shang (2022). "Zentropy Theory for Positive and Negative Thermal Expansion". In: *Journal of Phase Equilibria and Diffusion* 43.6, 598–605. issn: 1547-7037, 1863-7345. doi: 10.1007/s11669-022-00942-z.

Mongalo, L, A S Lopis and G A Venter (2016). "Molecular dynamics simulations of the structural properties and electrical conductivities of CaO–MgO–Al2O3–SiO2 melts". In: *Journal of NonCrystalline Solids* 452.15, pp. 194–202.

Muller, J, J H Zietsman and P C Pistorius (2015). "Modeling of Manganese Ferroalloy Slag Properties and Flow During Tapping". In: *Metallurgical and Materials Transactions B* 46.2, 2639–2651. issn: 1543-1916. doi: 10.1007/s11663-015-0426-7.

OpenAI (2023). *GPT-4 Technical Report*. technical report. OpenAI. url: https://arxiv.org/ pdf/2303.08774.pdf (visited on 08/02/2024).

Pelton, A.D. and M. Blander (1986). "Thermodynamic analysis of ordered liquid solutions by a modified quasichemical approach – Application to silicate slags". In: *Metallurgical and Materials Transactions B* 17B, pp. 805–815.

Roos, W A, A E J Bogaers and J H Zietsman (2023). "Geometric acceleration of complex chemical equilibrium calculations — Performance in two- to five-component systems". In: *Calphad* 82, p. 102584. issn: 03645916. doi: 10.1016/j.calphad.2023.102584.

Roos, W A and J H Zietsman (2022). "Geometric acceleration of complex chemical equilibrium calculations — Algorithm and application to two- and three-component systems". In: *Calphad* 77, p. 102420. issn: 03645916. doi: 10.1016/j.calphad.2022.102420.

Roscoe, R (1952). "The viscosity of suspensions of rigid spheres". In: *British Journal of Applied Physics* 3, pp. 267–269.

Schupsky, J P et al. (2020). "Viscosity and crystal morphology data of anorthite bearing synthetic coal slag systems". In: *Fuel* 280, p. 118663. issn: 0016-2361. doi: 10.1016/j.fuel.2020.118663. url: https://www.sciencedirect.com/science/article/ pii/S0016236120316598.

The Decoder (11 July 2023). *GPT-4 architecture, datasets, costs and more leaked*. url: https://the-decoder.com/gpt-4-architecture-datasets-costs-and-more-leaked/ (visited on 08/02/2024).

Thibodeau, E, A E Gheribi and I-H Jung (2016a). "A Structural Molar Volume Model for Oxide Melts Part I: Li2O-Na2O-K2O-MgO-CaO-MnO-PbO-Al2O3-SiO2 Melts—Binary Systems". In: *Metallurgical and Materials Transactions B* 47.2, 1147–1164. issn: 1543-1916. doi: 10.1007/s11663-015-0548-y.

– (2016b). "A Structural Molar Volume Model for Oxide Melts Part II: Li2O-Na2O-K2O-MgO-CaO-MnO-PbO-Al2O3-SiO2 Melts—Ternary and Multicomponent Systems". In: *Metallurgical and Materials Transactions B* 47.2, 1165–1186. issn: 1543-1916. doi: 10.1007/s11663-015-0543-3.

– (2016c). "A Structural Molar Volume Model for Oxide Melts Part III: Fe Oxide-Containing Melts".In: *Metallurgical and Materials Transactions B* 47.2, 1187–1202. issn: 1543-1916. doi: 10.1007/s11663-015-0549-x.

Thibodeau, E and I-H Jung (2016). "A structural electrical conductivity model for oxide melts". In: *Metallurgical AND Materials Transactions B* 47, 355–383.

Wimmer, G, A Fleischander and B Voraberger (2023). "Green Transition of the Iron and Steel Industry Impact on Slags and By-Products". In: *ce/papers* 6.6. doi: 10.1002/cepa.2954.

Wu, G et al. (2015). "Viscosity model for oxide melts relevant to fuel slags. Part 1: Pure oxides and binary systems in the system SiO2–Al2O3–CaO–MgO–Na2O–K2O". In: *Fuel Processing Technology* 137, pp. 93–103. issn: 0378-3820. doi: 10.1016/j.fuproc.2015.03. 025. url: https://www.sciencedirect.com/science/article/pii/S0378382015001472.

Zietsman, J H and P C Pistorius (2006). "Modelling of an ilmenite-smelting DC arc furnace process". In: *Minerals Engineering* 19. doi: 10.1016/j.mineng.2005.06.016.

Zietsman, J H, A Steyn and W Pretorius (2018). "Evaluating pre-treatment and smelting options with EMSIM to improve production efficiency". In: *Proceedings of INFACON XV*. Cape Town, South Africa: Southern African Institute of Mining and Metallurgy.